



# Early phases of the Galaxy from the chemical imprint on the iron-poor stars J0815+4729 and J0023+0307

J. I. González Hernández<sup>1,2</sup>, David S. Aguado<sup>3,6,1</sup>, Carlos Allende-Prieto<sup>1,2</sup>, Adam Burgasser<sup>4</sup>, and Rafael Rebolo<sup>1,2,5</sup>

<sup>1</sup> Instituto de Astrofísica de Canarias, E-38200 La Laguna, Tenerife, Spain  
e-mail: jonay.gonzalez@iac.es

<sup>2</sup> Universidad de La Laguna, Dept. Astrofísica, E-38206 La Laguna, Tenerife, Spain

<sup>3</sup> Dipartimento di Fisica e Astronomia, Università degli Studi di Firenze, Via G. Sansone 1, I-50019 Sesto Fiorentino, Italy

<sup>4</sup> Center for Astrophysics and Space Science, University of California San Diego, La Jolla, CA 92093, USA

<sup>5</sup> Consejo Superior de Investigaciones Científicas, E-28006 Madrid, Spain

Received: 118-11-2022; Accepted: 19-12-2022

## Abstract.

We have been exploring large spectroscopic databases such as SDSS to search for unique stars with extremely low iron content with the goal of extracting detailed information from the early phases of the Galaxy. We recently identified two extremely iron-poor dwarf stars J0815+4729 (Aguado et al. 2018b) and J0023+0307 (Aguado et al. 2018a) from SDSS/BOSS database and confirmed from high-quality spectra taken with ISIS and OSIRIS spectrographs at the 4.2m WHT and 10.4m GTC telescopes, respectively, located in La Palma (Canary Islands, Spain). We have also acquired high-resolution spectroscopy with UVES at 8.2m VLT telescope (Paranal, ESO, Chile) and HIRES at the 10m KeckI telescope (Mauna Kea, Hawaii, USA), uncovering the unique abundance pattern of these stars, that reveal e.g. the extreme CNO abundances in J0815+4729 with ratios  $[X/Fe] > 4$  (González Hernández et al. 2020). In addition, we are able to detect Li at the level of the lithium plateau in J0023+0307 (Aguado et al. 2019a), whereas we are only able to give a Li upper-limit 0.7 dex below the lithium plateau in J0815+4729, thus adding more complexity to the cosmological lithium problem. New upcoming surveys such as WEAVE, 4MOST and DESI will likely allow us to discover new interesting extremely iron-poor stars, that will certainly contribute to our understanding of the Early Galaxy, and the properties of the first stars and the first supernovae.

**Key words.** cosmology: observations – Galaxy: halo – primordial nucleosynthesis – stars: abundances – stars: Population II – stars:Population III – Galaxy:abundances – Galaxy:formation

## 1. Introduction

Extremely metal-poor stars must have formed from a mixture of material from the primordial nucleosynthesis and matter ejected from the first supernovae. Those stars are relics of the early epochs of the Milky Way, so their chemical composition, especially those still on the main sequence, holds crucial information such as the properties of the first stars and the early chemical enrichment of the Universe.

During the last decades, there has been an enormous observational effort to search for extremely metal poor stars in large spectroscopic surveys, such as Hamburg/ESO (HE; Christlieb et al. 2001), or Sloan Digital Sky Survey (SDSS; York et al. 2000), or narrow-filter photometric surveys such as Skymapper (Keller et al. 2007) or Pristine (Starkenburg et al. 2017). However, in the Galaxy with a few hundred thousand million stars, 1 over about 800 stars have  $[\text{Fe}/\text{H}] < -3$  in the solar neighbourhood, and we only know 14 stars at metallicity  $[\text{Fe}/\text{H}] < -4.5$  and only seven at  $[\text{Fe}/\text{H}] < -5$ . Almost all stars at  $[\text{Fe}/\text{H}] < -4.5$  are carbon-enhanced metal-poor (CEMP) stars with carbon abundances  $A(\text{C}) > 5$  dex (see Fig. 4), with the clear exception of the dwarf star J1029+1729 at  $[\text{Fe}/\text{H}] = -4.7$  (Caffau et al. 2011). At metallicities  $[\text{Fe}/\text{H}] < -5$ , these seven stars appear to be concentrated in the low carbon band where all are expected to be CEMP with no enrichment in n-capture elements (CEMP-no) with  $[\text{Ba}/\text{Fe}] < 1$  (Bonifacio et al. 2018). Thus, they belong to the CEMP-no class where their stellar abundances should reflect the pristine material polluted with the ejecta of core-collapse supernovae of a few zero metallicity massive stars.

## 2. Observations and analysis

We have extensively explored the SDSS/BOSS (Eisenstein et al. 2011) spectroscopic database and found several tens of extremely metal poor stellar candidates. Among these we discovered two extremely iron poor stars, J0815+4729 and J0023+0307, that we observed using with ISIS and OSIRIS

spectrographs at the WHT and GTC telescopes in the *Observatorio del Roque de los Muchachos* (La Palma, Canary Islands, Spain). In Fig. 1 we display these very high quality medium-resolution WHT/ISIS and GTC/OSIRIS spectra of these two chemically primitive stars that allowed us to confirm J0815+4729 as an extreme carbon enhanced star (Aguado et al. 2018b) and J0023+0307 as an hyper metal poor with apparently no carbon enhancement from the WHT/ISIS spectrum (Aguado et al. 2018a). The GTC/OSIRIS spectrum of J0815+4729 shows a forest of CH features together with the series of Balmer lines and a tiny Ca II K line. The WHT/ISIS of J0023+0307 shows also a tiny Ca II K feature but does not show any signature of carbon. We were able to reproduce fairly well the observed spectra with synthetic spectral fits using the FERRE code (see e.g. Aguado et al. 2017). The global analysis uses FERRE with a grid of synthetic spectra code ASS $\epsilon$ T (Koesterke et al. 2008) and model atmospheres from Kurucz ATLAS 9 (Mészáros et al. 2012).

We observed these two very faint targets using HIRES and UVES at the Keck and VLT telescopes, to get high resolution spectra ( $R \sim 37,500$  for HIRES and  $R \sim 31,000$  for UVES) with the goal of extracting the detailed chemical patterns of these two unique stars. A dedicated analysis of individual spectral features is performed using ATLAS9 model atmospheres and the 1D local thermodynamic equilibrium (LTE) using the SYNPLE code for spectral synthesis. We also use an automated fitting tool based on the IDL MPFIT routine, with continuum location, global shift, abundance, and global FWHM as free parameters (González Hernández et al. 2020).

The individual 1D spectra were corrected for barycentric and radial velocity, normalized, merged and binned into a single 1D spectrum of each star. In Fig. 2 we compare these high-quality spectra with those UVES spectra of other extremely iron-poor unevolved stars. Here we see clearly the huge amount of carbon in the spectrum of J0815+4729 as compared to J0023+0307 and other CEMP stars. We also clearly see the Ca II HK features in all these stars. We were able to

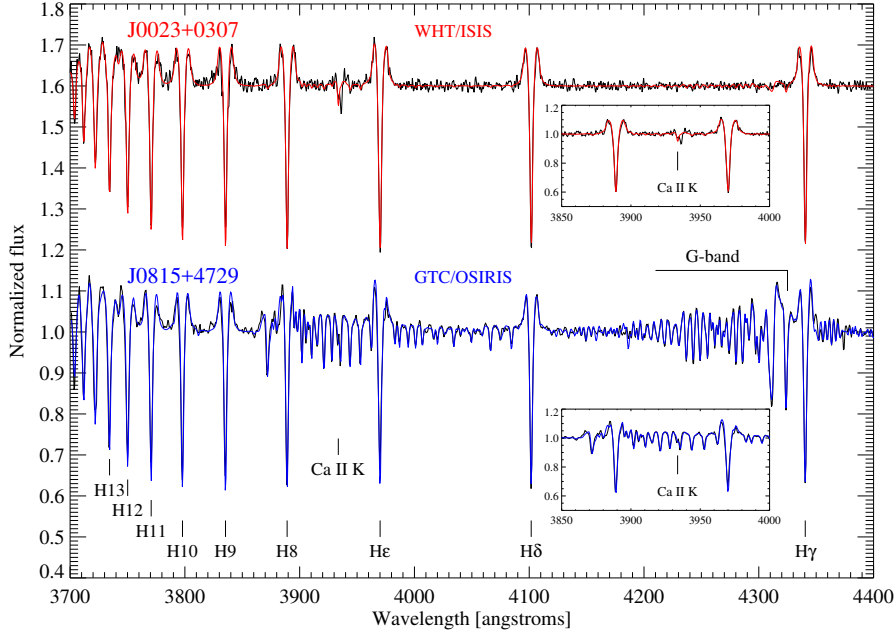


**Fig. 1.** WHT/ISIS spectrum of J0023+0307 and GTC/OSIRIS spectrum J0815+4729 (black lines) and the best fits obtained with FERRE (red and blue lines), normalized using a running-mean filter. The inner small panels show details of the Ca II K region for both stars.

measure a Ca abundance from Ca II lines of  $A(\text{Ca}) = 0.66$  in J0023+0307 significantly lower than the Ca abundance of  $A(\text{Ca}) = 1.60$  in J0815+4729, as compared to  $A(\text{Ca}) = 1.35$  of other two extremely iron poor unevolved C-enhanced stars J1035+0641 (Bonifacio et al. 2015) and HE 1327–2326 (Frebel et al. 2008). Given the similarity of stellar parameters of the stars shown in Fig. 2, the direct comparison of spectra and 1D-LTE element abundances seems quite reasonable. These high-quality spectra allowed us to measure an iron abundance of  $[\text{Fe}/\text{H}] = -5.5$  in J0815+4729 but only an upper-limit of  $[\text{Fe}/\text{H}] < -6.1$  (assuming  $[\text{Ca}/\text{Fe}] > 0.4$ ) in J0023+0307. Similarly to J0313–6708 (Keller et al. 2014) or J1035+0641, no iron lines were detected in the UVES spectrum. We note that the abundance ratio  $[\text{Ca}/\text{Fe}]$  in J0815+4729 and HE 1327–2326 are 0.75 and 0.71, respectively, which may justify the assumption of  $[\text{Ca}/\text{Fe}] > 0.4$  in J0023+0307 and the

upper-limit of  $[\text{Fe}/\text{H}] < -6.1$ . In Table 1 we collect the detailed chemical abundances of J0815+4729 (González Hernández et al. 2020), J0023+0307 (Aguado et al. 2019a) and HE 1327–2326 (Frebel et al. 2008).

This UVES spectrum unveiled that the star J0023+0307 is indeed also a CEMP with an abundance from the weak CH G band at the  $\lambda\lambda 4295 - 4315 \text{ \AA}$  of  $A(\text{C}) = 6.2$  (Aguado et al. 2019a), thus providing a high C abundance ratio of  $[\text{C}/\text{Fe}] > 3.9$ . On the other hand, the HIRES spectrum of J0815+4729 is populated with many C features (see Fig. 2), most of them CH lines, thus claiming for a significant amount of carbon according to the relatively hot effective temperature of the star (only about 100 K cooler than that of J0023+0307). This led to the detection of several C molecular features, including CH, CN and  $\text{C}_2$ , providing different C abundances. We measured inconsistent 1D abundances of  $A(\text{C}) = 7.4$  dex and  $= 8.0$  from CH (G-band)

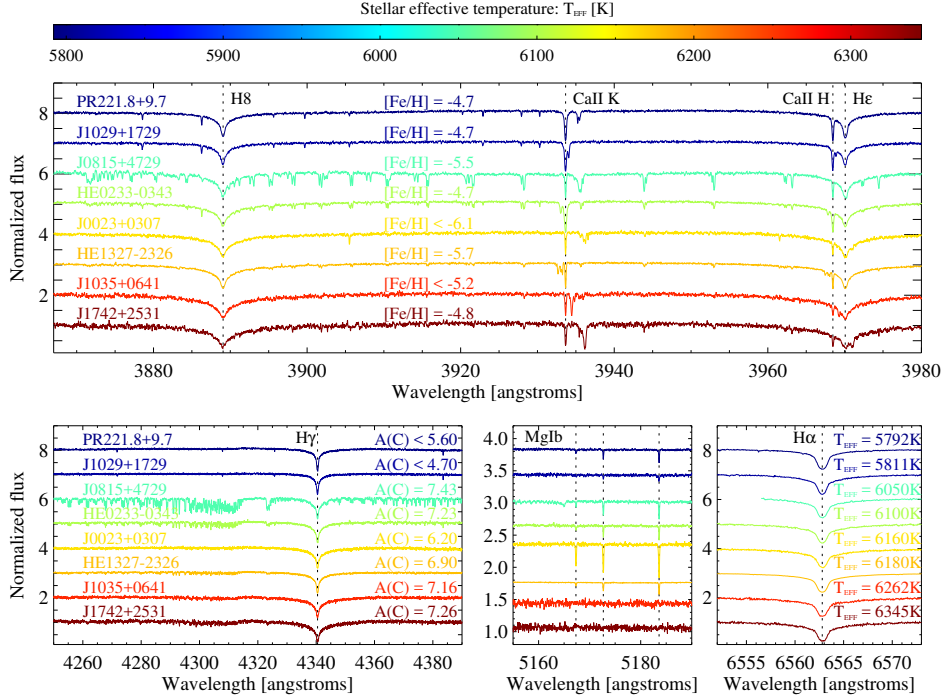


**Fig. 2.** High-resolution Keck/HIRES spectra of the star J0815+4729 together with the VLT/UVES spectra of other extremely iron-poor unevolved stars at  $[\text{Fe}/\text{H}] < -4.5$ . The spectra are sorted and colored by stellar effective temperature from top to bottom.

and the  $\lambda\lambda 163 - 5 \text{ \AA}$   $\text{C}_2$  molecular bands, respectively, as seen previously in the iron-poor cool giant HE 0107–5240 (Christlieb et al. 2004). We adopted the C abundance from CH as the reference C abundance of J0815+4729, providing a huge C abundance ratio of  $[\text{C}/\text{Fe}] = 4.5$ . The N and O abundances are also extremely enhanced in J0815+4729, leading to the first detection of the  $\lambda\lambda 3881 - 3 \text{ \AA}$  CN molecular band and the  $\lambda\lambda 7771 - 5 \text{ \AA}$  O I triplet in an ultra metal-poor unevolved star, with extreme abundance ratios of  $[\text{N}/\text{Fe}] = 4.4$  and  $[\text{O}/\text{Fe}] = 4.0$  (González Hernández et al. 2020).

The spectrum of J0023+0307 revealed high  $\alpha$ -element abundance ratios of  $[\text{Mg}/\text{Fe}] > 3.1$  and  $[\text{Si}/\text{Fe}] > 2.6$ , and also high odd-Z light element abundance ratios of  $[\text{Na}/\text{Fe}] > 1.9$  and  $[\text{Al}/\text{Fe}] > 2.0$ . The spectrum of J0815+4729 shows relatively lower ratios of  $[\text{Mg}/\text{Fe}] = 1.7$ ,

$[\text{Si}/\text{Fe}] < 1.3$ , and  $[\text{Ca}/\text{Fe}] = 0.75$ , but higher ratio of  $[\text{Na}/\text{Fe}] = 2.9$  and lower  $[\text{Al}/\text{Fe}] < 0.5$ . These differences show how unique are the abundance patterns of these stars, that are expected to be the result of a mixture of primordial matter with the ejecta of a few supernovae of the first massive stars formed in the first 300 Myr of Universe (Frebel & Norris 2015).

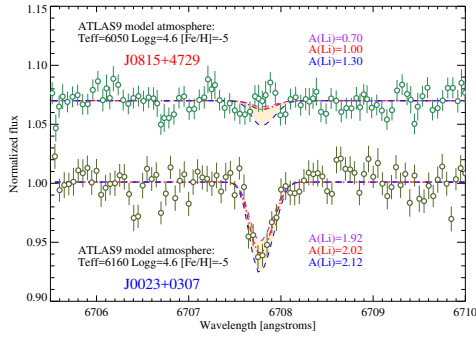
### 3. Discussion and conclusions

The detailed abundance patterns from C to Ni permitted a comparison with zero metallicity SN models, suggesting low-energy SN models with very little mixing of 21-27  $M_{\odot}$  Population III progenitors (Heger & Woosley 2010). The ratios of  $[\text{Sr}/\text{Fe}] < 1.0$  and  $[\text{Ba}/\text{Fe}] < 1.9$  in J0815+4729, do not allow to confirm this star as CEMP-no but the carbon abundance is compatible with the upper part of the low-carbon

**Table 1.** Element 1D LTE abundances of J0815+4729, J0023+0307 and HE 1327–2326

Element	$A_{\odot}(X)^{\dagger}$	J0815+4729		J0023+0307			HE 1327–2326			
		A(X)	[X/H] <sup>††</sup>	[X/Fe] <sup>††</sup>	A(X)	[X/H]	[X/Fe]	A(X)	[X/H]	[X/Fe]
Li	1.05	< 1.30	–	–	2.02	–	–	< 0.70	–	–
C	8.43	7.43	–1.00	4.49	6.20	–2.23	> 3.87	6.90	–1.53	4.18
N	7.83	6.75	–1.08	4.41	–	–	–	6.79	–1.04	4.67
O	8.69	7.23	–1.46	4.03	–	–	–	6.84	–1.85	3.86
Na	6.24	3.68	–2.56	2.93	2.08	–4.16	> 1.94	2.99	–3.25	2.46
Mg	7.60	3.77	–3.83	1.66	4.60	–3.00	> 3.10	3.54	–4.06	1.65
Al	6.45	< 1.50	< –4.95	< 0.54	2.35	–4.10	> 2.00	1.90	–4.55	1.16
Si	7.51	< 3.30	< –4.21	< 1.28	4.05	–3.46	> 2.64	–	–	–
Ca	6.34	1.60	–4.74	0.75	0.66	–5.68	> 0.42	1.34	–5.00	0.71
Ti	4.95	< 0.70	< –4.25	< 1.24	–0.42	–5.37	> 0.73	–0.09	–5.04	0.67
Cr	5.64	< 1.50	< –4.14	< 1.35	< 1.54	< –4.10	> 2.00	< 0.45	< –5.19	< 0.52
Fe	7.50	2.01	–5.49	–	< 1.40	< –6.10	–	1.79	–5.71	0.00
Ni	6.22	< 1.90	< –4.32	< 1.17	< 2.93	< –3.29	> 2.81	0.73	–5.49	0.22
Sr	2.87	< –1.60	< –4.47	< 1.02	< –1.68	< –4.55	> 1.55	–1.76	–4.63	1.08
Ba	2.18	< –1.40	< –3.58	< 1.91	< –1.33	< –3.51	> 2.59	< –2.14	–4.32	< 1.39

Notes:

† Solar abundances from Asplund et al. (2009):  $A_{\odot}(X) = \log \epsilon_{\odot}(X) = \log[N_{\odot}(X)/N_{\odot}(H)] + 12$ †† Element abundances with respect to solar values:  $[X/H] = A(X) - A_{\odot}(X)$ ,  $[X/Fe] = [X/H] - [Fe/H]$ **Fig. 3.** Lithium features (green dots with error bars) in high-resolution spectra of the star J0815+4729 (upper Keck/HIRES spectrum) and the star J0023+0307 (lower VLT/UVES spectrum) compared to SYNPLE synthetic spectra (the best-fit abundance is shown as red dashed-dotted lined).

band (see Fig. 4). The upper-limits in Sr, Ba and Fe do not allow to extract any conclusion in J0023+0307 that also appears to be located in the lower part of the low-carbon band. The only few stars known at  $[Fe/H] < -5$  suggest that all belong to this low-carbon band and may be CEMP-no stars, that are expected to form at the early phases of the Galaxy and their atmospheric abundances resemble the mixture of primordial matter with

the ejecta of a few metal-free weak SNe. There is so far no evidence for RV variations as well as no chemical signature of mass transfer from companion AGB stars in J0023+0307 and J0815+4729. Recently, Aguado et al. (2022) have performed a systematic survey of these extremely iron poor stars using the ultra-stable high-resolution ESPRESSO spectrograph (Pepe et al. 2021). ESPRESSO observations demonstrated the binarity of the cool iron-poor giant star HE 0107–5240 at  $[Fe/H] = -5.4$  but found a very high  $^{12}C/^{13}C$  ratio, thus supporting that this star remains as an unmixed CEMP-no with  $A(C) = 6.8$  located in the low-C band.

Finally, these iron-poor stars allow us to look back to the time to the big bang through the lithium abundances, in particular, in unevolved stars where Li can still survive in their atmospheres during the whole age of the Universe (see Fig. 2). The star J0023+0307 is particular interesting because it shows a significant Li feature at 6707.8 Å, with a metallicity of  $[Fe/H] < -6.1$ , thus the only star with a clear Li detection in this metallicity regime (see Fig. 3). The Li abundance of  $A(Li) = 2.0$  in J0023+0307 is at the level of the Li plateau (see Fig. 4), thus extending the upper envelope of the Li abundances in metal

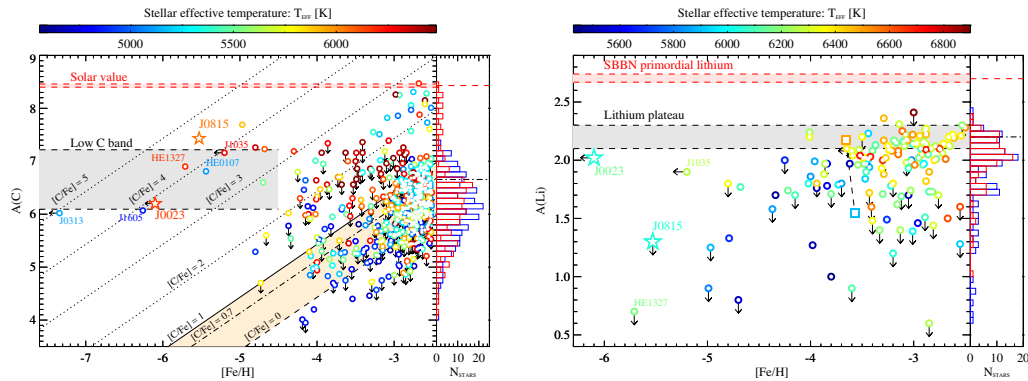


**Fig. 4.** *Left panel:* Carbon abundance vs.  $[\text{Fe}/\text{H}]$  of the stars J0815+4729 and J0023+0307 (large star symbols) compared with literature measurements for metal poor stars with  $[\text{Fe}/\text{H}] < -2.5$ . *Right panel:* Lithium abundance vs.  $[\text{Fe}/\text{H}]$  of the stars J0815+4729 and J0023+0307 (large star symbols) compared with literature measurements for unevolved metal poor stars with  $[\text{Fe}/\text{H}] < -2.5$  and  $\log g > 3.0$ . The two large squares connected with a black dashed line correspond to the metal-poor binary CS 22876–032 AB (González Hernández et al. 2008, 2019). In both panels, the literature data include those in González Hernández et al. (2020, and references therein) plus data in Yong et al. (2013); Hansen et al. (2015, 2016); Aguado et al. (2019b) for C, and those new and updated Li abundances in Kielty et al. (2021); Lardo et al. (2021); Matas Pinto et al. (2021). Stars with  $[\text{Fe}/\text{H}] < -5$  are labelled, including J0023+0307 and J0815+4729. Symbols are colored by their corresponding effective temperature. Downward and left-pointing arrows indicate upper limits.

poor stars downwards by several order of magnitude in metallicity, and keeping unresolved the discrepancy between the Li abundances in metal poor stars ( $A(\text{Li}) \sim 2.2$ ; Spite & Spite 1982; Rebolo et al. 1988) and the primordial Li abundance ( $A(\text{Li}) \sim 2.7$ ; Coc & Vangioni 2017) predicted from the standard Big Bang Nucleosynthesis at the very beginning of the Universe.

#### Affiliations

<sup>6</sup> INAF-Osservatorio Astrofisico di Arcetri, Largo E. Fermi 5, I-50125 Firenze, Italy

*Acknowledgements.* JIGH, CAP and RR acknowledge financial support from the Spanish Ministry of Science and Innovation (MICINN) project PID2020-117493GB-I00. DA acknowledges support from the ERC Starting Grant NEFERTITI H2020/808240.

#### References

Aguado, D., Molaro, P., Caffau, E., et al. 2022, arXiv e-prints, arXiv:2210.04910

- Aguado, D. S., Allende Prieto, C., González Hernández, J. I., & Rebolo, R. 2018a, *ApJ*, 854, L34
- Aguado, D. S., González Hernández, J. I., Allende Prieto, C., & Rebolo, R. 2017, *A&A*, 605, A40
- Aguado, D. S., González Hernández, J. I., Allende Prieto, C., & Rebolo, R. 2018b, *ApJL*, 852 L20
- Aguado, D. S., González Hernández, J. I., Allende Prieto, C., & Rebolo, R. 2019a, *ApJ*, 874, L21
- Aguado, D. S., Youakim, K., González Hernández, J. I., et al. 2019b, *MNRAS*, 490, 2241
- Asplund, M., Grevesse, N., Sauval, A. J., & Scott, P. 2009, *ARA&A*, 47, 481
- Bonifacio, P., Caffau, E., Spite, M., et al. 2015, *A&A*, 579, A28
- Bonifacio, P., Caffau, E., Spite, M., et al. 2018, *A&A*, 612, A65
- Caffau, E., Bonifacio, P., François, P., et al. 2011, *Nature*, 477, 67
- Christlieb, N., Green, P. J., Wisotzki, L., & Reimers, D. 2001, *A&A*, 375, 366

- Christlieb, N., Gustafsson, B., Korn, A. J., et al. 2004, *ApJ*, 603, 708
- Coc, A. & Vangioni, E. 2017, *International Journal of Modern Physics E*, 26, 1741002
- Eisenstein, D. J., Weinberg, D. H., Agol, E., et al. 2011, *AJ*, 142, 72
- Frebel, A., Collet, R., Eriksson, K., Christlieb, N., & Aoki, W. 2008, *ApJ*, 684, 588
- Frebel, A. & Norris, J. E. 2015, *ARA&A*, 53, 631
- González Hernández, J. I., Aguado, D. S., Allende Prieto, C., Burgasser, A. J., & Rebolo, R. 2020, *ApJ*, 889, L13
- González Hernández, J. I., Bonifacio, P., Caffau, E., et al. 2019, *A&A*, 628, A111
- González Hernández, J. I., Bonifacio, P., Ludwig, H.-G., et al. 2008, *A&A*, 480, 233
- Hansen, C. J., Nordström, B., Hansen, T. T., et al. 2016, *A&A*, 588, A37
- Hansen, T., Hansen, C. J., Christlieb, N., et al. 2015, *ApJ*, 807, 173
- Heger, A. & Woosley, S. E. 2010, *ApJ*, 724, 341
- Keller, S. C., Bessell, M. S., Frebel, A., et al. 2014, *Nature*, 506, 463
- Keller, S. C., Schmidt, B. P., Bessell, M. S., et al. 2007, *PASA*, 24, 1
- Kielty, C. L., Venn, K. A., Sestito, F., et al. 2021, *MNRAS*, 506, 1438
- Koesterke, L., Allende Prieto, C., & Lambert, D. L. 2008, *ApJ*, 680, 764
- Lardo, C., Mashonkina, L., Jablonka, P., et al. 2021, *MNRAS*, 508, 3068
- Matas Pinto, A. M., Spite, M., Caffau, E., et al. 2021, *A&A*, 654, A170
- Mészáros, S., Allende Prieto, C., Edvardsson, B., et al. 2012, *AJ*, 144, 120
- Pepe, F., Cristiani, S., Rebolo, R., et al. 2021, *A&A*, 645, A96
- Rebolo, R., Beckman, J. E., & Molaro, P. 1988, *A&A*, 192, 192
- Spite, M. & Spite, F. 1982, *Nature*, 297, 483
- Starkenburger, E., Martin, N., Youakim, K., et al. 2017, *MNRAS*, 471, 2587
- Yong, D., Norris, J. E., Bessell, M. S., et al. 2013, *ApJ*, 762, 26
- York, D. G., Adelman, J., Anderson, Jr., J. E., et al. 2000, *AJ*, 120, 1579